Iraqi Journal of Science

ISSN: 0067-2904

Analysis of the Interference Pattern of the Fiber Interferometer and employing it as a Motion Sensor

Duraid H. Ahmed*[1], Musab S. Mohammed[2], Fathi M. Jasim[2]
[1]Department of Science, College of Basic Education, University of Mosul, Iraq
[2]Department of Physics, College of Education for pure science, University of Mosul, Iraq

Received: 5/12/2019 Accepted: 15/3/2020

Abstract

The production and analysis of an optimal interference pattern for the optical fiber interferometer of a 193.1THz continuous laser source was simulated. This was achieved by comparing the spectral spectroscopy of the two arms of the interferometer, to be used as a heterodyne detector, in sensing the body range, speed, and direction of movement by delaying the time between the arms.

The study showed that it is possible to make calculations through the interference model to give a range of 1.5, 3, and 4.5 mm using free spectral range (FSR) of 0.1, 0.05, and0.03 THz and velocity of 77625, 38812, and 23287 m/s, by the Doppler shift in frequency (Δf) of 0.1, 0.05, and 0.03 THz, respectively. Also, distancing or approaching of bodies was determined by increasing or decreasing the fringe spatial frequency (FSF).

Keywords: Optical Interferometer; Laser Doppler Velocimetry; Fiber optic Sensor; Heterodyne detection system.

تحليل نمط التداخل لمقياس التداخل الليفي وتوظيفه كمتحسس للحركة

دريد حازم احمد الهلالي[1]* ، مصعب صالح محمد[2] ، فتحي محمد جاسم[3]
[1]قسم العلوم, كلية التربية الأساسية, جامعة الموصل, نينوى,العراق
[2]قسم الفيزياء, كلية التربية للعلوم الصرفة, جامعة الموصل, نينوى,العراق

الخلاصة

تم محاكاة إنتاج وتحليل نمط التداخل الأمثل لمصدر ليزر مستمر تردده 193.1THz لمقياس التداخل الليفي و مقارنة طيفي اذرع المقياس لتوظيفه في الكشف المتجانس للتحسس بمدى وسرعة واتجاه جسم متحرك عن طريق تغيير التأخير الزمني بين ذراعي المقياس.

أظهرت الدراسة أن من الممكن عمل حسابات من خلال نموذج التداخل لتعطي تصور عن بعد الجسم (1.5 , 3 , 4.5) mm عبر المدى الطيفي الحر FSR (0.03 , 0.05 , 0.1)THz وسرعة الجسم (23287 , 38812 , 77625) m/s بإزاحة دوبلر في التردد Δf (0.03 , 0.05 , 0.1)THz . فضلا عن تحديد ابتعاد الجسم او اقترابه بزيادة او نقصان التردد المكاني للهدب FSF.

Introduction

Laser Doppler Velocimeters (LDVs) are very precise sensors for measuring movement across a big field of frequencies. LDVs accuracy depends on the interference measurement. The body movement under the test is automatically converted into the fringe shift [1].

*Email: duraidhahmed@uomosul.edu.iq

The ideal model of fringe is achieved in practical interferometers via a coherent wave transmitted by separate paths due to the wave of light to generate constructive and deconstructive fringes at sequential spatial points due to different optical pathways and phase differences [2].

Interferometers are classified, according to the number of overlapping optical beams, into two-beam or multiple-beam devices. The most common interferometers are the Fizeau, the Michelson, the Mach – Zehnder and the Sagnac interferometers, while the most well-known multi-beam device is the Fabry-Perot interferometer [3-4].

Optic fiber interferometric sensors have been used in wide practical applications such as monitoring of mechanical deformation of aircrafts, bridges. and buildings, as well as biomedical sensitization to health monitoring systems [4].

Optical fiber was used as a sensor through a heterodyne detection technique, which depends on optical interference of pressure sensing, stress, temperature, rotation, velocity measurement of particles, as well as sensitivity in the electrical and magnetic fields [5-8]. In the heterodyne detection system, a reference laser beam is introduced to measure the Doppler direct frequency as a result of the optical interference of the reference wave with the reflective wave which is reflected by the particle. It is also applied to improve the resolution of measured frequency strength, increase the accuracy by reduction of the beat frequency, and reduce the size of the interference area and then improve the accuracy of spatial analysis of measurement [9-10].

The objective of this study is to simulate a perfect optical interference model by using the delay interferometer and continuous laser, as a high-coherence source. The package of Optisystem programs is used as a sensor to measure the range, the velocity, and the direction of the body by analyzing the spectral distribution of the interference generated, based on the effect of time delay between the arms of the interferometer.

Theory

The optical interference spectrum can be described as a modified intensity based on the wavelength of the optical spectrum and the result of the phase differences between the optical beams. The peaks of the modified spectrum mean that beams are in phase and out-of-phase, in the modulus of 2π [4]. Since the interferometers give a lot of temporal and spectral information as their beams, the measurement can be determined by various changes in the wavelength, intensity, frequency, phase and so on. Hence, they can give remarkable performance in large dynamic range, high sensitivity, and high accuracy [4].

A phase difference of 2π rad (for constructive interference) corresponds to the optical path difference (OPD) of λ . The mathematical relation between path difference δ and phase difference ϕ was described by the ratio $\frac{\delta}{\lambda} = \frac{\phi}{2\pi}$, which gives [7]:

$$\phi = \frac{2\pi}{\lambda}\delta \qquad \text{----------(1)}$$

In LDVs which are based on heterodyne detection system, a reference laser beam is introduced to directly measure the beat frequency of the Doppler shift as a heterodyne result of high interference with the light scattered by the particle. It is also applied to improve the frequency measurement resolution and accuracy as the signal frequency is reduced and to improve the measurement spatial resolution [9, 10].

Particle velocity V was calculated by measuring the Doppler frequency f_d , or transit time of the particle passing through a fringe $\tau = 1 / f_d$ (Figure-1) [10]

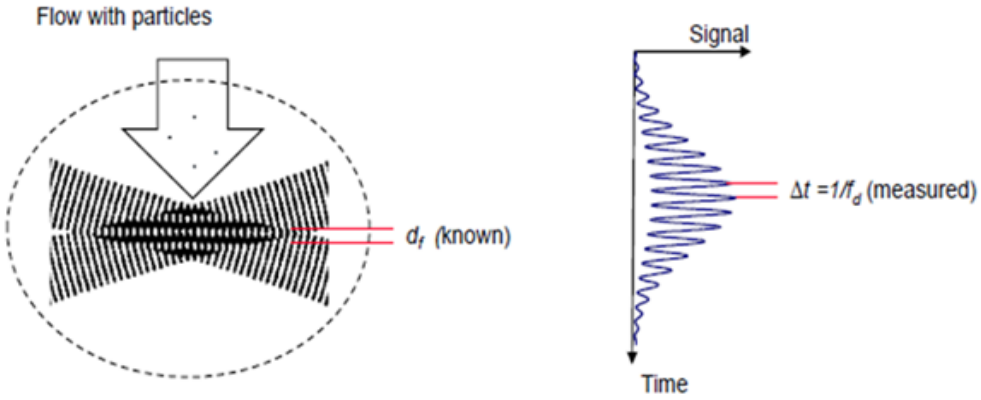

Figure 1-Fringe pattern and signal burst. Image courtesy: Dantec Dynamics [10].

$$V = \frac{f_d \ \lambda}{2 \sin\theta} \quad \text{--------(2)}$$

$$V = \frac{d_f}{\tau} = d_f \times f_d \quad \text{--------(3)}$$

where d_f is the fringe spacing or fringe separation and θ is the angle between two beams [9]. Equation (2) does not specify the direction of speed. Thus, in order to solve this problem one of the two interference beams is shifted, by Bragg frequency known as f_B, practically ~ 40MHz, using the Bragg cell, to become the equation (2), as shown in the equation (4). If the Doppler frequency increases, this gives an indication of the object's approximation and vice versa.

$$V = \frac{(f_d + f_B)\lambda}{2 \sin\theta} \quad \text{-------(4)}$$

In standard dual beam configuration, an LDV system is not able to differentiate the traveling direction of a particle . From the fringe theory, the still fringe pattern within the same probe will be in motion after one of the laser beams is frequency shifted by some mechanical-optical or electric-optical means [11]. The fringe motion makes the difference in Doppler frequencies in opposite directions across the probe volume [11].

Figure-2 shows the delay interferometer which consists of two independent arms, the reference and the sensing arms. Fiber coupler splits the light into the two arms, which is then recombined by another fiber coupler. Because of the presence of optical path difference between the arms, optical interference will occur at the recombined. For sensing purposes, the reference arm is maintained for external changes and the variable or sensing arm remains exposed to external changes. This can be sensitive to temperature, stress, and refractive index changes [12].

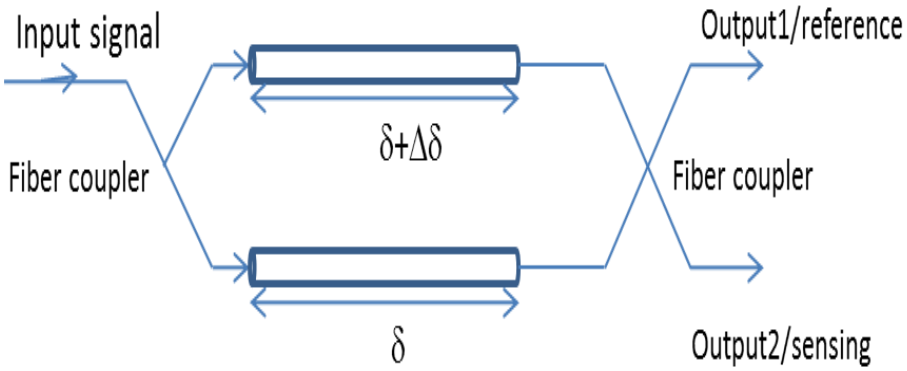

Figure 2- General schematic of the optical delay interferometer [12].

Results and Discussion:-

Figure-3 shows the schematic diagram for light interference production by delay interferometer.

The continuous laser frequency of 193.1 THz was the source with 0 dBm as a coherence source ideal for interference. The specifications of the used interferometer are listed in Table-1.

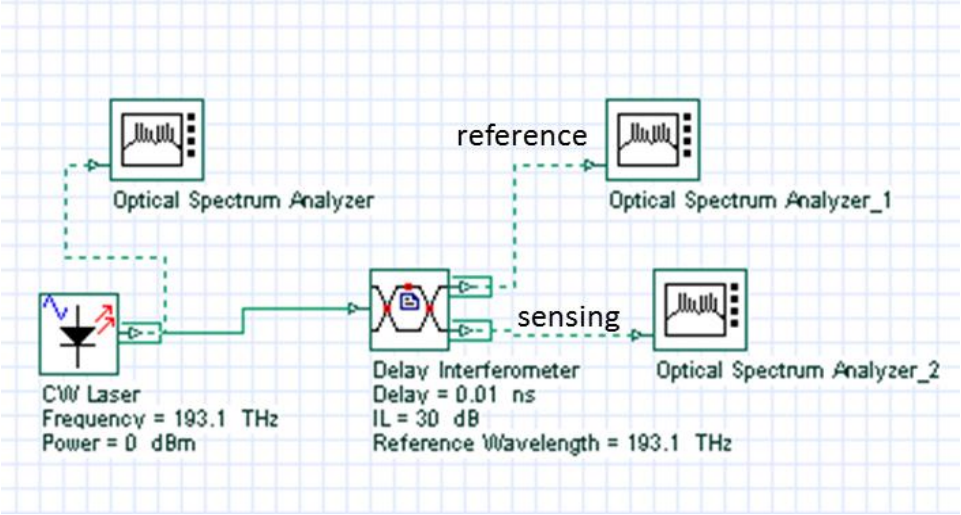

Figure 3-Schematic diagram for light interference production by optical fiber interferometers

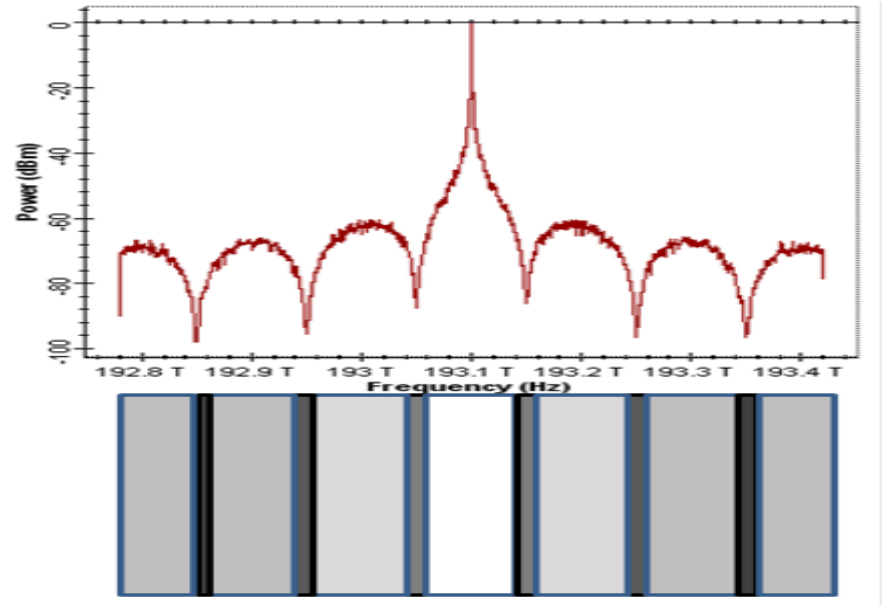

Figure 4-The spectrum of CW monochromatic laser source with a maximum power 0 dBm at 193.1 THz

Table 1-Specification parameters of delay interferometer [12]

Parameters	Value
Delay Time	0.01 ns
PDF, Polarization-dependent frequency shift	700 MHz
IL, Maximum insertion loss	30 dB
PDL, Polarization-dependent loss	0.05 dB
Additional loss	0. 35 dB
Reference frequency	193.1THz
Reference wavelength	1552.5nm

Figure-4 shows the spectrum of the continuous monochromatic laser displayed by optical spectrum analyzer with a maximum power 0dBm at 193.1THz and by a resolution of 0.01 ns. The time delay τ between the two arms was fixed around 0.01 ns. Figure-5 shows the spectrum of interference at the reference output within a spectral range of 192.8-193.4 THz. It is consisting of seven luminous fringes

with the same width and variable intensity separation by a frequency of 0.1THz symmetrical about the maximum intensity of the zero-order fringe at 193.1THz, within a spectral range of 193.05-193.15 THz. Furthermore, six dark fringes of similar width and variable intensity.

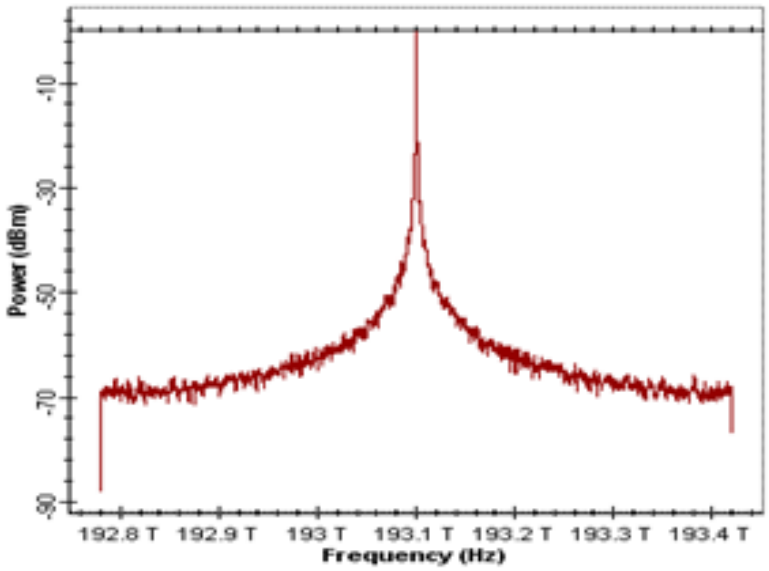

Figure 5-The spectrum of interference at reference output of the interferometer.

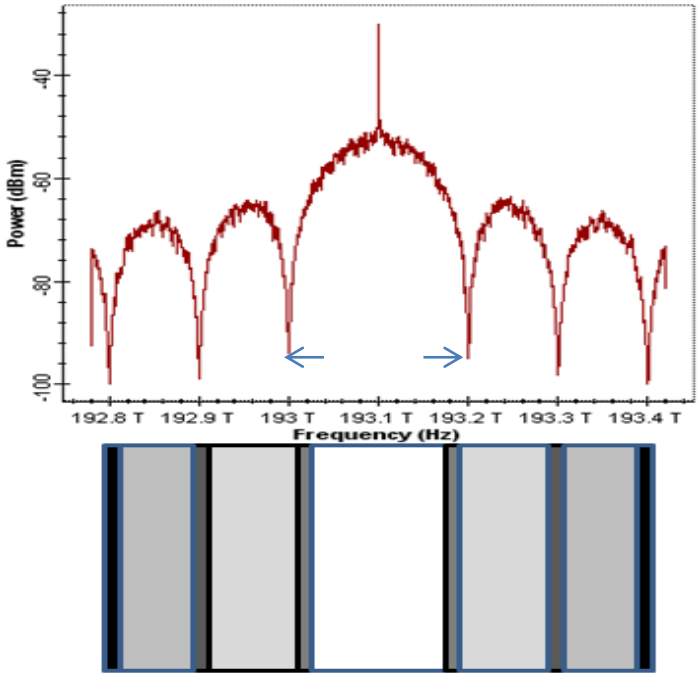

Figure 6- The spectrum of interference at sensing output of the interferometer

Figure-6 presents the spectrum of interference at the sensing output within the same range of the spectrum. Note that the spectral pattern is affected by the time delay. The shift in the fringes by the inverted time delay, and thus the maximum intensity positions of the lateral illuminations in Figure-5, was changed by dark positions in Figure-6. Also, the luminous fringes were degrade to become five, with the dark position is confirmed and the zero fringe width is doubled and shifted into various regions of the spectrum (193 -193. 2 THz). Therefore, the path difference was calculated as the change in the width of the zero fringe. As a result, the central fringe increased by the inverted time delay between the arms of the interferometer. Also, time delay appears as a frequently spatial difference of

intensity. However, the free spectral range "FSR" and the interval adjacent fringes for both figures are constant, based on the inverted time delay only. Table-2 shows data for the interferometer output.

Table 2-Interference parameter data for the reference and sensing output of the interferometer

Reference output	Sensing output	
Bandwidth for zero-order fringe	(193.05-193.15)THz	(193-193.2)THz
Luminous fringes number	7	5
Dark fringes number	6	6
FSR =ΔF	0.1THz	0.1THz

To obtain more details about the parameters of this fringe model and to benefit from it later, we used some known mathematical relationships in calculating these parameters, as follows: [1]
Fringe Spatial Frequency (FSF) = $\frac{\text{OPD}}{\lambda}$ = τ F = 0.01ns ×193.1THz =1931 rad^{-1}

Free Spectral Range (FSR) = $\frac{c}{OPD} = \frac{1}{\tau} = \frac{1}{0.01\ ns}$= 0.1THz

Fringe Spacing = 1/ FSF = FSR / F = 1/1931= 0.000517 rad .

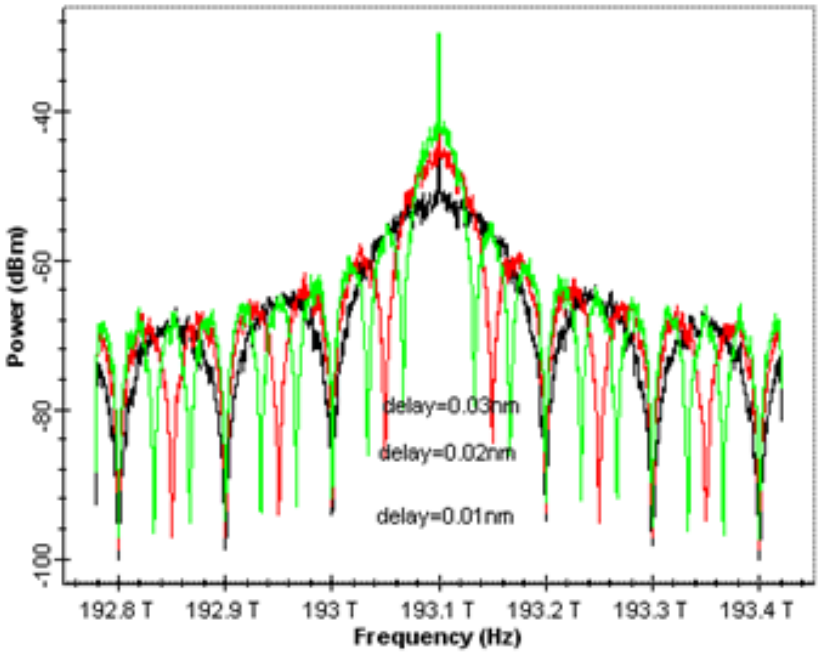

Figure 7-The interference spectrum at sensing output of the interferometer for three time delays (0.01ns, 0.02ns, and 0.03ns).

Figure-7 shows the changes in the frequency modification of the interference pattern for three times delays (0.01, 0.02, 0.03 ns). It is clear from the figures that the number of spectral fringes increases with the delay between the interfering beams. It is also shown that the central width of zero-order fringe is reduced as the time delay is increased. Figure-7 is similar to the case of monitoring the movement of a target in the case of distancing or approaching. As the time delay increases, the body moves away and the path difference is increased further. The fringe spatial frequency increases and the fringes spacing decreases and, thus, the number of fringes is increased, and vice versa.

It is also possible to take into consideration the FSR, frequency shift (ΔF), as a means of sensing the body range. It gives an indication of the time delay and then of the optical path difference, which is rewarded as twice as the body range. The vibration of the fringes is sensitive to the body movement. As can be seen from Figure-7, signals with FSR = 0.1THz, 0.05THz, and 0.03THz are equivalent to time delays of 0.01nm , 0.02nm , and 0.03nm , representing OPD = 3mm, 6mm, and 9mm , which is corresponding to three ranges of 1.5mm, 3mm , and 4.5mm , respectively. Also, the fringe spacing expresses the Doppler shift in frequency, according to the equation: [8]

$FS = \frac{FSR}{F} = \frac{\Delta F}{F} = \frac{2V}{c}$

where V is body velocity. Thus, the velocities according to Figure-7 are 77680 m/s , 38840 m/s , 25634 m/s for delays of 0.01ns , 0.02ns, 0.03ns , respectively. Table-3 shows all data related to the use of the interference spectrum of Figure-7 as a motion sensor.

Table 3-Data of the interference spectrum used as a motion sensor

Time delay	FSR=ΔF	OPD	Range	Velocity	FSF	FS	Luminous fringes number
0.01ns	0.1 THz	3 mm	1.5 mm	77680 m/s	1931 Rad^{-1}	0.51 mrad	5
0.02ns	0.05 THz	6 mm	3 mm	38840 m/s	3862 Rad^{-1}	0.25 mrad	11
0.03ns	0.033 THz	9 mm	4.5 mm	25634 m/s	6372 Rad^{-1}	0.15 mrad	17

Conclusions

This study showed that it is possible to make calculations for the interference pattern to employ it as a motion sensor that provides information about the range of body, the velocity of body, and the movement direction. The results showed that the interference model was sensitive to the range by the FSR, to the velocity by the FS or Doppler frequency shift, and to the movement direction by the FSF . It is also concluded from the results of the interference spectrum that the increase in the number of fringes is an indication of the distancing the body, while the decrease indicates the approaching of the body. Finally, the interference spectrum was a successful and accurate sensor system for phase difference and frequency shift.

Acknowledgment

The authors are very grateful to the University of Mosul/ College of Basic Education for providing facilities which helped to improve the quality of this work.

References

1. Hussain B , Muhammad T, Rehan M , Aman H , Aslam M ,Ikram M ,et al. **2013**. Fast Processing of Optical Fringe Movement in Displacement Sensors Without Using an ADC. *Photonic Sensors* .2013**; 3**(3): 241–245.
2. John D. **2003**. Optical interferometry in astronomy. *Rep. Prog. Phys*. **66** (2003): 789-857 .
3. Hariharan P. **2003**. *Optical Instrument*. 2th ed. Elsevier/Academic Press: New York .2003.Chapter 21,Interferometers; p.21-1-21-28.
4. Bommareddi R. **2014**. Applications of Optical Interferometer Techniques for Precision Measurements of Changes in Temperature, Growth and Refractive Index of Materials. *J. Technologies*. 2014; **2**: 54-75.
5. Byeong H., Young H., Kwan S., Joo B., Myoung J, Byung S ,et al. **2012**. Interferometric Fiber Optic Sensors . *J. Sensors* . 2012 ; **12**: 2467-2486.
6. Dhurandhar S., Ni T. and Wang G. **2013**. Numerical simulation of time delay interferometry for a LISA-like mission with the simplification of having only one interferometer . Class. Quantum Grav. 2013.
7. U. Sharma & X. Wei, Fiber Optic Interferometric Devices, Springer Science+Business Media New York 2013.
8. Serway, R.A. and Jewett, J.W**. 2010**. *Physics for Scientists and Engineers with Modern Physics*, 8th ed., Brooks/Cole engage learning, USA.
9. Yariv, A. and Yeh, p. **2007**. *Photonics: Optical Electronics in Modern Communications* ,6th ed. ,Oxford University Press.
10. Arakeri, J.H. **2017**. *Experimental Methods* , Indian Institute of Science, Bangalore, India-560012.
11. Zhu, J.Y. **1966**. Laser Doppler Velocimetry for Flow Measurements in Pulp and Paper Research, TAPPI Engineering Conference Chicago, Illinois,1996.
12. Opti System Component Library Optical Communication System Design Software. Version.7,US, Copyright © 2008 Optiwave .